

Sol-Gel Fabricated $\text{CoFe}_2\text{O}_4/\text{SiO}_2$ Nanocomposites: Synthesis and Magnetic Properties

Jana Vejpravová¹, Jiří Plocek^{2,3}, Daniel Nižňanský^{2,3}, Alžběta Hutlová⁴, Jean L. Rehspringer^{4,5}, and Vladimír Sechovský¹

¹Charles University in Prague, Faculty of Mathematics and Physics, Department of Electronic Structures, 121 16-Praha 2, Czech Republic

²Charles University in Prague, Faculty of Natural Sciences, Department of Inorganic Chemistry, 128 40-Praha 2, Czech Republic

³Institute of Inorganic Chemistry, Academy of Sciences of the Czech Republic, 250 68-Řež, Czech Republic

⁴I.P.C.M.S., Groupe des Matériaux Inorganiques, F-67037 Strasbourg Cedex, France

⁵Charg de recherche au CNRS IPCMS-GMI UMR 7504 CNRS/Université Louis Pasteur, BP 2367034 Strasbourg Cedex 2, France

Well-defined CoFe_2O_4 nanoparticles embedded in an amorphous SiO_2 matrix have been synthesized by a sol-gel method, characterized and investigated by Mössbauer spectroscopy and magnetic properties measurements. The mean particle size increases from 3 to 15 nm consistently with the temperature of the subsequent annealing, which varied from 800°C to 1100°C, respectively. The composites exhibit superparamagnetic behavior with the blocking temperature T_B increasing with the mean particle size from 80 to 350 K, respectively. Sufficiently high value of $H_c \sim 2.5$ T (at 2 K) has been observed for the sample annealed at 1100°C.

Index Terms—Ferrite nanoparticles, sol-gel method, superparamagnetism.

DUE to expected applications of nanoparticles, the demand for their manufacture rises despite persistent difficulties in larger-scale production. So far, many studies of elemental nanoparticles (Ni, Co, Fe) have been published, e.g., [1] and [2], while overall reports on ferrite-based systems are still few in number. One reason is that to obtain isolated ferrite nanoparticles is often a crucial problem, due to difficult control of the particle shape and size distribution [3]. Promising candidates are cobalt ferrite composites because of high coercivity fields H_c and saturated magnetization M_s values provided [4], [5]. In this paper, we present details of fabrication, characterization, and selected magnetic characteristics of well-defined CoFe_2O_4 nanoparticles embedded in an amorphous SiO_2 matrix.

We used a conventional sol-gel method with tetraethyl-orthosilicate (TEOS), HNO_3 as an acid catalyst, formamide as a modifier, and methanol as a solvent for silica matrix preparation. $\text{Fe}(\text{NO}_3)_3 \cdot 9\text{H}_2\text{O}$ and $\text{Co}(\text{NO}_3)_2 \cdot 6\text{H}_2\text{O}$ were first dissolved in methanol, and the Si/Fe molar ratio was fixed to 100/15 (gelation time ~ 24 h at 40°C). The samples were left two days for ageing, followed by progressive drying at 40°C for three days in a flowing N_2 atmosphere. After drying, the samples were preheated at 300°C in a vacuum for 2 h, and then under atmospheric pressure at one of the following temperatures: 800°C, 900°C, 1000°C, or 1100°C, and finally labeled according to the last annealing temperature as S800–S1100, respectively.

A high-resolution transmission electron microscope, Topcon, was used for the direct observation of the particle appearance. Particle-size determination was done using the Scion Images software. The nanocomposites show well-defined grains, with the increasing mean particle size from 3 nm up to 15 nm in diam-

TABLE I
SUMMARY OF MAGNETIC CHARACTERISTICS: BLOCKING TEMPERATURES T_B [DETERMINED FROM AC SUSCEPTIBILITY, T_{diff} , T_{max} , (1)], AVERAGE MAGNETIC MOMENT PER PARTICLE μ , AVERAGE PARTICLE DIAMETER (R) OBTAINED BY THE FIT OF THE WEIGHTED SUM OF LANGEVIN FUNCTIONS (L), MEAN PARTICLE DIAMETER OBSERVED BY TEM AND FROM FWHM, EXTRAPOLATED COERCIVITY FIELD H_{C0}

Sample	T_B (K) AC	T_B (K) diff	T_B (K) T_{max}	T_B (K) eq. (1)
S800	87	92	50	80
S900	107	116	60	105
S1000	290	305	180	275
S1100	x	350	300	295
Sample	μ (μ_B) L	R (nm) L	R (nm) TEM/FWHM	H_{C0} eq. (1)
S800	4700	1.5/2	1.5	1.9
S900	5700	2/3	2	1.8
S1000	8100	5.5/4	5.5	2.2
S1100	8700	7.5/8	7.5	2.9

eter, according to the annealing temperature for the S800–S1100 samples, respectively. See Table I.

All samples were characterized by powder X-ray diffraction (XRD) using a Siemens D500 diffractometer equipped with a cobalt anode ($\lambda(\text{CoK}\alpha) = 1.7890 \text{ \AA}$) and a quartz primary monochromator in order to identify the phase composition. The XRD patterns of the samples after final thermal treatment are shown in Fig. 1. A tendency of crystallization as a function of the heating temperature is reflected by a broad diffraction peak at around 25° (2θ). The process of crystallization as a function of the heating temperature can be followed from the full width at half maximum (FWHM) of diffraction peaks, which follows the Scherrer equation, and it also permitted us to estimate the particle size, see Table I [6]. The Mössbauer spectra measurement was done in the transmission mode with ^{57}Co diffused into a Rh matrix as the source, moving with constant acceleration. The

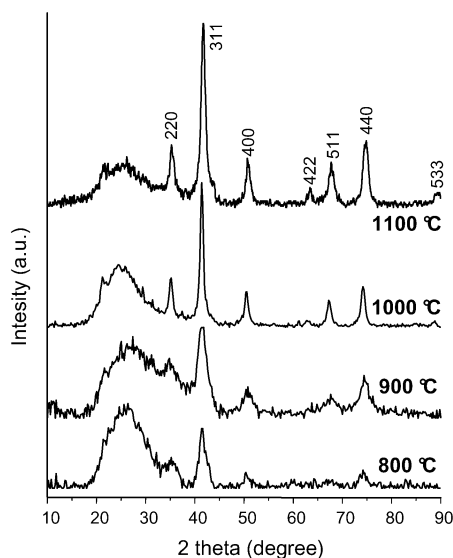


Fig. 1. XRD patterns of S800–S1100 samples.

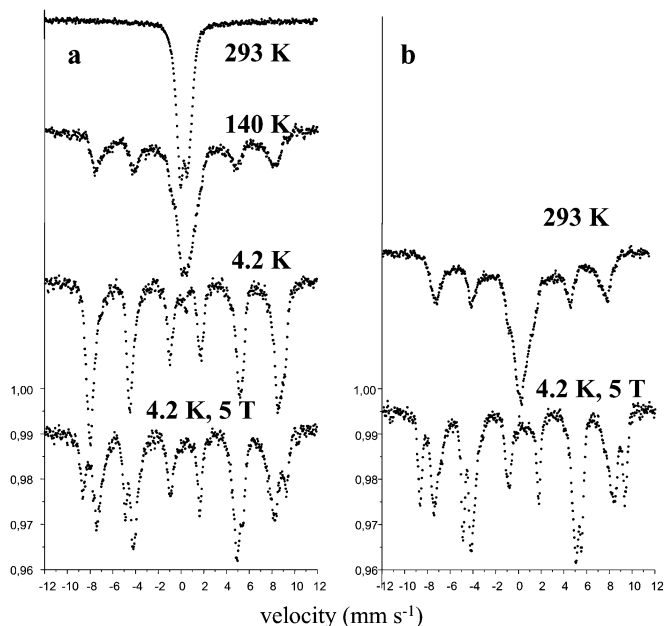


Fig. 2. Comparison of Mössbauer spectra of S900 (a) and S1000 (b) recorded at zero magnetic field and at 5 T at selected temperatures.

spectrometer was calibrated by means of a standard α -Fe foil, and the isomer shift was expressed with respect to this standard at 293 K. The spectra were recorded at several different temperatures in magnetic fields up to 5 T, applied perpendicular to the direction of the γ -ray emission and fitted with the help of the NORMOS program. The temperature development of the spectra of S900 is shown in Fig. 2(a). The sample is superparamagnetic (SPM) at room temperature (no sextet is observed), while after cooling to 140 K, partial magnetic arrangement is observed (sextet appearance). Simultaneous occurrence of both the sextet and the doublet reflects a certain size distribution of the CoFe_2O_4 particles. At 4.2 K, complete ferromagnetic ordering of the magnetic moments in Co ferrite particles is observed. Due to a very strong overlap of the subspectra, one cannot distinguish between iron positions in the spinel structure (Td-tetra-

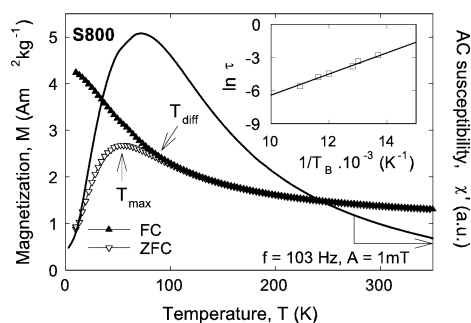


Fig. 3. Temperature dependence of ZFC-FC magnetization of S800 sample at 50 mT in comparison with that of AC susceptibility (real part, χ'). The inset shows the logarithmic dependence of the relaxation time τ against the inverse blocking temperature T_B , according to the Néel–Arrhenius law.

hedral, Oh-octahedral sites). When we take generally accepted recoilless factors for the spinel structure ($f_{\text{Td}} : f_{\text{Oh}} = 1.2$) [7] into account, we can express the real formula of our spinel as $(\text{Co}_{0.41}\text{Fe}_{0.59})[\text{Co}_{0.59}\text{Fe}_{1.41}]\text{O}_4$. Great deviation from the ideal structure can be explained by the presence of very small particles and significant influence of surface atoms. The spectra of the S1000 sample are represented in Fig. 2(b). Simultaneous occurrence of both sextet and doublet can be explained by a certain size distribution of the CoFe_2O_4 particles reflecting a partly ferromagnetic sample at 293 K. At 4.2 K in 5 T, the spectrum shows a magnetically ordered structure of cobalt ferrite (no doublet is present). Moreover, there is again a deviation from the ideal inverse spinel structure (area ratio ($S_{\text{Td}} : S_{\text{Oh}}$) differs from 1.2).

The DC magnetization (M) as a function of temperature (2–350 K) and magnetic field (0–14 T), together with the AC susceptibility (frequency range 83–8333 Hz, DC amplitude 1 mT), were measured in the PPMS 14 T and PPMS 9 T devices (Quantum Design, San Diego, CA). The temperature dependencies of the DC magnetization were measured at 50 mT; first after cooling the sample in a zero magnetic field (ZFC curve), followed by cooling the sample under an applied magnetic field (FC curve) and measuring during heating at the same field. The furcation of ZFC and FC curves at a certain temperature (denoted as T_{diff} in our case) is one of the characteristic features of an SPM system, as seen in Fig. 3 for S800. However, the coinciding broad maximum observed on the ZFC curve occurs at a slightly lower temperature (symbolized as T_{max}) than T_{diff} . Such behavior usually signals a certain particle-size distribution in the nanocomposite; while a fraction of the largest particles already freeze at T_{diff} , the majority fraction of the nanoparticles in the sample is being blocked at T_{max} , resulting in a distribution of the blocking temperatures T_B in the sample; the distinctive values (at T_{diff} and T_{max} , respectively) of the blocking temperatures T_B for all four samples are summarized in Table I. The value of T_{max} and T_{diff} monotonously increases with the increasing mean size of the particles (corresponding to the higher annealing temperatures) as expected; for the S1000 and S1100 samples, the maximum on the ZFC curve at T_{diff} becomes less pronounced than for S800 and S900, respectively. At low temperatures, the value of coercivity field H_c (symmetric for opposite polarity of magnetic field $H_c = -H_c$) is increasing with increasing size of particles

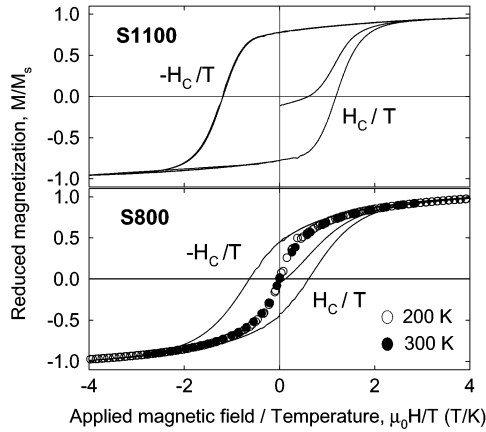


Fig. 4. Virgin magnetization curves and hysteresis loops of S800 and S1100 samples measured at 2 K (solid line), together with unhysteretic curves of S800 in SPM state.

(despite a slightly varying value of saturated magnetization from $M_s \sim 19 \text{ Am}^2\text{kg}^{-1}$ for S1100 to $M_s \sim 16 \text{ Am}^2\text{kg}^{-1}$ for S800 at 2 K), see Fig. 4. At low temperatures, coercivity of a system of noninteracting and randomly oriented particles is expected to follow the relation

$$H_C(T) = H_{C0} \left[1 - \left(\frac{T}{T_B} \right)^{1/2} \right]. \quad (1)$$

An extrapolated value of H_{C0} , together with T_B (summarized in Table I) have been derived for all samples. The T_B values are appreciably consistent with those obtained from temperature dependencies of the DC magnetization and the AC susceptibilities, as shown later. An estimation of nanoparticle mean radius was obtained using general formulas

$$T_B = \frac{K \langle V \rangle}{25 k_B} \quad (2)$$

where K is the first-order magneto-crystalline anisotropy constant of bulk CoFe₂O₄ ferrite [8], supposed to be temperature-independent, $\langle V \rangle$ is the average particle volume ($\mu = M_s^{\text{bulk}} \langle V \rangle$), M_s^{bulk} is the saturated magnetization of bulk CoFe₂O₄, and T_B and k_B have the usual meaning. The values of radii of the nanoparticles are in a good agreement with those obtained by other performances.

Finally, the SPM behavior above T_B has been confirmed when plotting M/M_s versus $\mu_0 H/T$ (M_s is the saturated magnetization at the corresponding temperature), resulting in a universal curve (see Fig. 4). This scaling is consistent with the SPM response; the contribution from the SPM nanoparticles to the total magnetization can be described as a weighted sum of Langevin functions [1], [9], [10] providing a mean particle diameter, distribution width, and mean magnetic moment per particle, respectively (see Table I for results).

The temperature dependence of the AC susceptibility shows characteristic maxima corresponding to the blocking temperatures T_B [11] (derived from the maximum position at 103 Hz are summarized in Table I), which are shifted to higher temperatures with increasing frequencies. This observation corroborates the idea that nanoparticles behave like noninteracting and single-domain species, excluding any additional dipole-dipole or interparticle interactions. The linear dependence of $\ln f$ (f is the frequency of AC field 83–8333 Hz) versus $1/T_B$ follows the Néel–Arrhenius law [11] $\tau = \tau_0 \times e^{[E_a/k_B T]}$, where τ is the relaxation time, E_a is the anisotropy energy barrier, and τ_0 ranges from 10^{-9} to 10^{-11} s for SPM systems. The resulting values of τ_0 and E_a are 1.8×10^{-8} s and 1.3×10^{-8} s; 1227 K and 920 K for the S800 and S900 samples, respectively. The values of τ_0 are rather close to the ones expected for an ideal SPM system, indicating almost negligible interparticle interactions in the composite. In summary, we have prepared a series of CoFe₂O₄ nanocomposites embedded in an amorphous SiO₂ matrix. Nonhomogeneous occupation of Fe positions in the structure has been observed by the Mössbauer spectroscopy under magnetic field. Magnetic behavior of the composites follows the Néel theory of single-domain noninteracting entities exhibiting SPM behavior above T_B increasing with the temperature of the heat treatment according to the mean particle size. Below T_B , appreciably high values of coercivity develop, increasing up to H_{C0} 2.9 T for S1100.

ACKNOWLEDGMENT

This work is a part of the research program MSM0021620834, financed by the Ministry of Education of the Czech Republic. This work was also supported by the Grant Agency of the ASCR under Project KJB4032402.

REFERENCES

- [1] F. C. Fonseca, G. F. Gya, R. F. Jardim, R. Muccillo, N. L. V. Carreno, E. Longo, and E. R. Leite, *Phys. Rev. B*, vol. 66, no. 10, pp. 104406–104411, 2002.
- [2] A. Fnidiki, C. Dorien, F. Richomme, J. Teillet, D. Lemarchand, N. H. Duc, J. B. Youssef, and H. Le. Gall, *J. Magn. Magn. Mater.*, vol. 262, no. 3, pp. 368–373, 2003.
- [3] L. D. Tung, V. Kolesnichenko, D. Caruntu, N. H. Chou, C. J. O'Connor, and L. Spinu, *J. Appl. Phys.*, pt. 2, vol. 93, pp. 7486–7488, 2003.
- [4] A. Hutlová, D. Nižňanský, J.-L. Rehspringer, C. Estournes, and M. Kurmoo, *Adv. Matt.*, vol. 15, no. 19, p. c5305+, 2003.
- [5] R. D. K. Misra, S. Gubbala, and A. Kale, *Mater. Sci. Eng. B*, vol. 111, no. 2–3, pp. 164–174, 2004.
- [6] R. Jenkins and R. L. Snyder, *Introduction to X-ray Powder Diffraction*. New York: Wiley, 1996.
- [7] J. L. Dormann, D. Fiorani, and S. Vitticoli, *Proc. Int. Conf. Applic. Mossbauer Effects (Jaipur)*. New Delhi, India, 1981, p. 206.
- [8] S. Krupička, *Fyzika feritu a přibuzných kysličníků*. Praha, Czech Republic: Academia, 1980.
- [9] E. F. Ferrari, F. C. S. da Silva, and M. Knobel, *Phys. Rev. B*, vol. 56, no. 10, pp. 6068–6093, 1997.
- [10] J. C. Cezar, M. Knobel, and H. C. N. Tolentino, *J. Magn. Magn. Mater., Special Issue on SI*, pt. 2, vol. 226, pp. 1519–1521, 2001.
- [11] L. Néel, *Ann. Geophys. (CNSR)*, vol. 5, p. 99, 1949.